A Closed-Form Solution for Image Warping of Mesh in Quad-Tree Representation

Chih-Cheng Wei, Chin-Hsing Chen, Jin-Yuan Wang
Department of Electrical Engineering, National Cheng Kung University, Taiwan
E-mail: weisuper@ms31.hinet.net

摘要

四分樹的架構常被用來依據影像的特性分割一個影像成大小不同的區域。在四分樹的架構下，一個區域可能連結超過四個節點，因而有三種類型的節點產生。在本論文中，我們推導三類型節點的控制率計算公式，對於影像形彎從非規則網格到非規則網格，我們提出中介一個規則網格的新方法。利用此方法，影像形彎從規則或非規則網格到目標網格可以藉由是否中介一個規則網格並利用我們所推導的控制率計算公式來完成。如此我們推導的控制率公式提供在四分樹架構下，網格影像形彎的公式解。實驗結果顯示使用我們提出的方法可以得到高的視訊品質。

關鍵詞：四分樹，網格，影像形彎。

Abstract

The quad-tree structure has often been used to decompose an image into regions of different size based on image properties. In quad-tree structure, one patch might be attached more than four nodes and three types of nodes may be generated. In this paper, we derived a closed-form control rate formula for each type of nodes. For the image warping starting from a non-regular mesh to a target non-regular mesh, we proposed a novel indirect method in which an intermediate regular mesh is inserted. By this method, the image warping starting from either a regular or a non-regular mesh to a target mesh can be accomplished by using the derived closed-form control rate formula with/without inserting a regular mesh between the starting mesh and the target mesh. Thus, the control-rate formula we derived offer a closed-form solution for image warping of mesh in quad-tree representation. Experiments showing that high-quality video can be reconstructed by using our proposed method.

Keywords: quad-tree, mesh, image warping.

1. Introduction

Motion compensation is used to reduce temporal redundancy in video compression and the block-matching algorithm (BMA) is the most popular technique used for motion estimation. But there are some drawbacks in BMA: 1) it cannot handle image rotations and scaling and 2) it cannot preserve the neighboring relations between the blocks, resulting in blocking artifacts [10]. A new motion compensation method named “Mesh” was developed in MPGE-4 to overcome the drawbacks in the BMA and offer high compression rate. In the mesh-based coding scheme, motion compensation within each mesh element is accomplished by more general spatial transformation related to the geometry of the mesh element [1, 2, 4, 7, 11]. The mesh method synthesizes image transfiguration /deformation with the motion trajectories of the node in the mesh thus offers a mechanism for video compression.

There are many ways to decompose an image into regions of different size based on image properties. For simple and regular implementation, quad-tree decomposition is a good choice. One patch might be attached more than four nodes after quad-tree decomposition. Therefore, a patch may be deformed from a rectangle to a polygonal. In this paper, we present a closed-form solution for image warping of mesh in quad-tree representation. We solved this problem by utilizing the concept of “control rate” at each node. There are three types of nodes generated. The warping effect caused by the “control rate” for the each type of nodes is derived and expressed in a closed form.

By this method the image warping from a regular mesh is simply accomplished by using the control rate of each node. For the image warping starting from a non-regular mesh to a target non-regular mesh, we proposed a novel indirect method in which an intermediate regular mesh is inserted and thus the warping can be accomplished by using the control rate formulae for the regular mesh.

The remaining sections of this paper are organized as follows. In section 2, an overview of mesh representation and quad-tree decomposition is presented. We drive the control rate formula used in the warping process for three types of nodes in section 3. Section 4 presents the outcomes of our simulations. Section 5 gives the conclusion.

2. Overview of Mesh Representation

2.1 Definition of 2D Mesh

Mesh is the generic term to describe a geometrical partition of an image domain into polygonal elements (e.g., triangles or quadrangles). A mesh is like a network that is represented as a collection of the same types of polygons, each polygon is named “patch”, and the vertexes of each polygon are named “node” [4]. A deformable mesh is a time-varying mesh in which each patch deforms in time while still forming a non-overlapping and complete covering of the underlying image domain as shown in Fig. 1. The displacement of a node controls the deformation of its associated patches. The deformation or mapping function over the entire mesh is interpolated from nodal trajectories in an element-by-element manner.

In the deformable mesh representation of an image sequence, a mesh is constructed for each frame in the sequence such that a mesh covers each frame. The mesh of the reference frame is deformed to generate a predictive frame that will match the objective frame as well as possible.

In general, two approaches to the selection of grid points from which frame can be taken. In the first approach, the grid points are selected from the previous frame and the motion is estimated by finding their best matches in the current frame. This scheme is referred as forward warping. In the second approach, the grid points are selected from the current image. The motion is estimated by finding the best match for these points in the previous frame. This scheme is referred as backward warping [5, 6, 8]. Fig. 2 illustrates the forward warping and the backward warping.

2.2 Quad-Tree Decomposition

The quad-tree structure has been frequently used for video processing and image compression [13]. Quad-tree decomposition recursively decomposes a rectangular image region into four quadrants (patches) and continues decomposing each of these quadrants (patches) into four sub-quadrants (sub-patches) until each sub-patch lives up to the non-decomposition condition. At the time when a patch is divided into four children-patches, the layer number of these children-patches is numbered as one plus the layer number of the parent patch. As shown in Fig. 3, after decomposition there are four old nodes and five new nodes in the original patch. The layer of these new nodes is defined as the same with that of the sub-quadrants. Fig. 4 illustrates a mesh in quad-tree representation.

3. Image Warping

Image warping from a regular mesh presented is accomplished by using the control rate of each node. But the calculation of the control rate of a node in a non-regular mesh is more complicated and an analytical formula is hard to obtain. In this paper, the image warping from a non-regular mesh is accomplished through an indirect method as follows. Fig. 5(a) showed a non-regular mesh and its deformed mesh, in which the image texture of the former is warped to the latter. The indirect method we proposed is illustrated in Fig. 5(b). Firstly the texture of an intermediate regular mesh is obtained from the Nth frame by backward warping that using the control rate of the intermediate regular mesh. Then the texture of the intermediate regular mesh is forward warped to produce the texture of the (N+1)th frame by using the control rate of the intermediate regular mesh. In each of the above two warping process, a regular mesh is always involved and therefore can be accomplished by using the control rate formulae for the regular mesh.

3.1 Three Types of Nodes

A node is associated with a motion vector and a control polygon which is the union of the rectangles that join the node. A node controls the deformation of the patches within its control polygon. The control polygon of a node is affected by the quad-tree decomposition process [3, 13]. Three types of nodes are defined in the mesh: the general node (GN), the special node (SN) and the boundary node (BN) [3]. As shown in Fig. 6, nodes in white are the GNs, nodes in black are the SNs and nodes in gray are BNs. A GN has four patches joining the node and the node is at the vertex of these patches. The four patches joining the node are of the same size. When the location of a node is on the boundary of an image frame and only one or two patches of the same size joins the node, the node is also defined as a GN. A SN is jointed by four patches of different size. When the location of a node is on the boundary of an image frame and only two patches of different size joins this node, the node is considered as SN. A BN has three patches joining the node and the node is located at the vertex of two patches and at the boundary of the other patch.

3.2 Bilinear Transformation for Image Warping

A spatial transformation defines a mapping relationship between a pixel position in the input and the corresponding one of the output image. The bilinear transformation functions is given by

$$T_x(x,y) = a_1xy + a_2x + a_3y + a_4$$
$$T_y(x,y) = b_1xy + b_2x + b_3y + b_4 \qquad (1)$$

where a_1~a_4 and b_1~b_4 denote the eight parameters of the transformation function. Since there are eight degrees of freedom, this transformation is used in a quadrilateral patch [6, 10]. Fig. 7 illustrates the bilinear transformation in which the vertexes (x_A,y_A), (x_B,y_B), (x_C,y_C), (x_D,y_D) of a quadrilateral patch of the Nth frame are mapped to (x'_A,y'_A), (x'_B,y'_B), (x'_C,y'_C), (x'_D,y'_D) of the (N+1)th frame by forward warping. We can use these corresponding points to solve the eight parameters of Eq. (1). Then the bilinear transformation function Eq. (1) can be used to calculate the mapped position for each pixel within the quadrilateral patch after the parameters of the equation have been solved. But, it is hard to solve these parameters. Fortunately, we can change the viewpoint from the position of each pixel to the motion vector of each pixel. Based on the motion vector viewpoint, we do not need to solve the equation parameters, and still achieve the same warping purpose [2, 6, 9]. The Eq. (1) can be transformed to the following form:

$$u(x,y) = CR_A(x,y)*u_A + CR_B(x,y)*u_B + CR_C(x,y)*u_C + CR_D(x,y)*u_D$$
$$v(x,y) = CR_A(x,y)*v_A + CR_B(x,y)*v_B + CR_C(x,y)*v_C + CR_D(x,y)*v_D \qquad (2)$$

where u(x,y)=x'-x and v(x,y)=y'-y denote the motion components at (x,y) in the horizontal and the vertical directions respectively. (u_A, u_B, u_C, u_D) and (v_A, v_B, v_C, v_D) denote the motion components in the horizontal and the vertical direction at the vertices of the quadrilateral patch as shown in Fig. 8.

In Eq. (2), the motion components at point (x,y) are regarded as the addition of the motion components at four vertexes multiplied with the corresponding coefficients [12]. The four coefficients are named the control rates of the four vertices within the patch. They are given by

$$CR_A(x,y) = \left(1 - \frac{(x-x_A)}{(x_C-x_A)}\right) * \left(1 - \frac{(y-y_A)}{(y_C-y_A)}\right)$$

$$CR_B(x,y) = \left(1 - \frac{(x-x_B)}{(x_D-x_B)}\right) * \left(1 - \frac{(y-y_B)}{(y_D-y_B)}\right)$$

$$CR_C(x,y) = \left(1 - \frac{(x-x_C)}{(x_A-x_C)}\right) * \left(1 - \frac{(y-y_C)}{(y_A-y_C)}\right)$$

$$CR_D(x,y) = \left(1 - \frac{(x-x_D)}{(x_B-x_D)}\right) * \left(1 - \frac{(y-y_D)}{(y_B-y_D)}\right) \qquad (3)$$

The value of the control rate ranges from 0 to 1. Fig. 9 shows the control rate from node A within a patch in which the brightest indicates the control rate 1 and the darkest indicates the control rate is 0.

3.3 The Control Rate of the Three Types of Nodes

In the following, the control rate for each type of node is calculated. The $CR^i_j(x,y)$ denotes the control rate of node j at position (x, y) in patch i.

(a). The control rate of a GN:

Fig. 10(a) shows a GN Q joined by four patches of equal size. The control polygon of node Q consists of four parts: patch "0"(DOQP), patch "1"(OERQ), patch "2"(QRHS) and patch "3"(PQSG) respectively. Since the four patches are of the same size, $CR^i_Q(x,y)$, i=0, 1, 2, 3 are simply given by

$$CR^0_Q(x,y) = \left(1 - \frac{(x-x_Q)}{(x_D-x_Q)}\right) * \left(1 - \frac{(y-y_Q)}{(y_D-y_Q)}\right)$$

$$CR^1_Q(x,y) = \left(1 - \frac{(x-x_Q)}{(x_E-x_Q)}\right) * \left(1 - \frac{(y-y_Q)}{(y_E-y_Q)}\right)$$

$$CR^2_Q(x,y) = \left(1 - \frac{(x-x_Q)}{(x_H-x_Q)}\right) * \left(1 - \frac{(y-y_Q)}{(y_H-y_Q)}\right)$$

$$CR^3_Q(x,y) = \left(1 - \frac{(x-x_Q)}{(x_G-x_Q)}\right) * \left(1 - \frac{(y-y_Q)}{(y_G-y_Q)}\right) \qquad (4)$$

Fig. 10(b) shows the control rate of node Q.

(b). The control rate of a SN:

Fig. 11(a) shows a SN L joined by four patches of different sizes. The control polygon of node L consists of four parts: patch “0”(BJLK), patch “1”(JCML), patch “2”(LMFN) and patch “3”(TLWV). Since the four patches joining node L are of different size, the control rate of L will be affected by nodes T and W. For this reason, $CR^{i}_{L}(x,y)$, i=0, 1, 2, 3 are determined according to the following three steps:

Step 1: Calculates $CR^{i}_{L}(x,y)$, i=0, 1, 2, 3 by neglecting the effect due to nodes T and W. That is,

$$
\begin{aligned}
CR_L^0(x,y) &= \left(1-\frac{(x-x_L)}{(x_B-x_L)}\right)*\left(1-\frac{(y-y_L)}{(y_B-y_L)}\right)\\
CR_L^1(x,y) &= \left(1-\frac{(x-x_L)}{(x_C-x_L)}\right)*\left(1-\frac{(y-y_L)}{(y_C-y_L)}\right)\\
CR_L^2(x,y) &= \left(1-\frac{(x-x_L)}{(x_F-x_L)}\right)*\left(1-\frac{(y-y_L)}{(y_F-y_L)}\right)\\
CR_L^3(x,y) &= \left(1-\frac{(x-x_L)}{(x_V-x_L)}\right)*\left(1-\frac{(y-y_L)}{(y_V-y_L)}\right)
\end{aligned}
\tag{5}
$$

The result is shown in Fig. 11(b) in which discontinuities are seen and the control rate of node L at nodes T and W are not zero.

Step 2: Calculate the control rate of node T in patch 0 and the control rate of node W in patch 2 that match the control rate produced by node L at T and W respectively. Because the layer of nodes T and W are one more than the layer of node L. The control area of T and W is smaller than the L does. Four points T’(x_{0T},y_{0T}), T”(x_{1T},y_{1T}), W’(x_{0W},y_{0W}) and W”(x_{1W},y_{1W}) are introduced to compute the control rate as shown in Fig. 11(a). That is,

$$
\begin{aligned}
CR_T^0(x,y) &= \left[CR_L^0(x_T,y_T)\right]*\left(1-\frac{(x-x_T)}{(x_{0T}-x_T)}\right)*\left(1-\frac{(y-y_T)}{(y_{0T}-y_T)}\right), \quad y \le y_T\\
CR_T^0(x,y) &= \left[CR_L^0(x_T,y_T)\right]*\left(1-\frac{(x-x_T)}{(x_{1T}-x_T)}\right)*\left(1-\frac{(y-y_T)}{(y_{1T}-y_T)}\right), \quad y > y_T\\
CR_W^2(x,y) &= \left[CR_L^2(x_W,y_W)\right]*\left(1-\frac{(x-x_W)}{(x_{0W}-x_W)}\right)*\left(1-\frac{(y-y_W)}{(y_{0W}-y_W)}\right), \quad x \le x_W\\
CR_W^2(x,y) &= \left[CR_L^2(x_W,y_W)\right]*\left(1-\frac{(x-x_W)}{(x_{1W}-x_W)}\right)*\left(1-\frac{(y-y_W)}{(y_{1W}-y_w)}\right), \quad x > x_W
\end{aligned}
\tag{6}
$$

Fig. 11(c) shows the control rate of node T in patch 0.

Step 3: Deduce the effects produced by nodes T and W from the control rate of node L. That is,

$$
\begin{aligned}
CR_L^0(x,y) &= \left(1-\frac{(x-x_L)}{(x_B-x_L)}\right)*\left(1-\frac{(y-y_L)}{(y_B-y_L)}\right)\\
&\quad -\left(1-\frac{(x_T-x_L)}{(x_B-x_L)}\right)*\left(1-\frac{(y_T-y_L)}{(y_B-y_L)}\right)*\left(1-\frac{(x-x_T)}{(x_{0T}-x_T)}\right)*\left(1-\frac{(y-y_T)}{(y_{0T}-y_T)}\right), \quad y \le y_T\\
CR_L^0(x,y) &= \left(1-\frac{(x-x_L)}{(x_B-x_L)}\right)*\left(1-\frac{(y-y_L)}{(y_B-y_L)}\right)\\
&\quad -\left(1-\frac{(x_T-x_L)}{(x_B-x_L)}\right)*\left(1-\frac{(y_T-y_L)}{(y_B-y_L)}\right)*\left(1-\frac{(x-x_T)}{(x_{1T}-x_T)}\right)*\left(1-\frac{(y-y_T)}{(y_{1T}-y_T)}\right), \quad y > y_T\\
CR_L^1(x,y) &= \left(1-\frac{(x-x_L)}{(x_C-x_L)}\right)*\left(1-\frac{(y-y_L)}{(y_C-y_L)}\right)\\
CR_L^2(x,y) &= \left(1-\frac{(x-x_L)}{(x_F-x_L)}\right)*\left(1-\frac{(y-y_L)}{(y_F-y_L)}\right)\\
&\quad -\left(1-\frac{(x_W-x_L)}{(x_F-x_L)}\right)*\left(1-\frac{(y_W-y_L)}{(y_F-y_L)}\right)*\left(1-\frac{(x-x_W)}{(x_{0W}-x_W)}\right)*\left(1-\frac{(y-y_W)}{(y_{0W}-y_W)}\right), \quad x \le x_W\\
CR_L^2(x,y) &= \left(1-\frac{(x-x_L)}{(x_F-x_L)}\right)*\left(1-\frac{(y-y_L)}{(y_F-y_L)}\right)\\
&\quad -\left(1-\frac{(x_W-x_L)}{(x_F-x_L)}\right)*\left(1-\frac{(y_W-y_L)}{(y_F-y_L)}\right)*\left(1-\frac{(x-x_W)}{(x_{1W}-x_W)}\right)*\left(1-\frac{(y-y_W)}{(y_{1W}-y_w)}\right), \quad x > x_W\\
CR_L^3(x,y) &= \left(1-\frac{(x-x_L)}{(x_V-x_L)}\right)*\left(1-\frac{(y-y_L)}{(y_V-y_L)}\right)
\end{aligned}
\tag{7}
$$

Fig. 11(d) shows the control rate of node L after considering the effect due to nodes T and W. The discontinuities of Fig. 11(b) are removed and the control rate of node L at nodes T and W are zero in Fig. 11(d).

(c). The control rate of a BN:

Fig. 12(a) shows a BN K joined by three patches of different size. According to the layer of node K, a point K’(x_{0K},y_{0K}) is placed for describing the control polygon of K. The control polygon of node K consists of three parts: patch “0”(K’BEO), patch “1”(BJLK) and patch “2”(KTVU). Since the three patches joining node

K are of different sizes, the control rate of K will be affected by nodes U and T. That is like the SN L affected by nodes T and W in the case (b). Four points U'(x_{0U},y_{0U}), U"(x_{1U},y_{1U}), T'(x_{0T},y_{0T}) and T"(x_{1T},y_{1T}) are generated to compute the control rate as shown in Fig. 12(a). $CR^{i}_{K}(x,y)$, i=0, 1, 2, are determined according to the three steps described in the case (b) and the results are given by

$$CR_K^0(x,y)=\left(1-\frac{(x-x_K)}{(x_{0K}-x_K)}\right)*\left(1-\frac{(y-y_K)}{(y_{0K}-y_K)}\right), \quad x \le x_K$$

$$\begin{aligned}CR_K^0(x,y)=&\left(1-\frac{(x-x_K)}{(x_O-x_K)}\right)*\left(1-\frac{(y-y_K)}{(y_O-y_K)}\right)\\&-\left(1-\frac{(x_U-x_K)}{(x_O-x_K)}\right)*\left(1-\frac{(y_U-y_K)}{(y_O-y_K)}\right)*\left(1-\frac{(x-x_U)}{(x_{0U}-x_U)}\right)*\left(1-\frac{(y-y_U)}{(y_{0U}-y_U)}\right)\end{aligned}, \quad x_K < x \le x_U$$

$$\begin{aligned}CR_K^0(x,y)=&\left(1-\frac{(x-x_K)}{(x_O-x_K)}\right)*\left(1-\frac{(y-y_K)}{(y_O-y_K)}\right)\\&-\left(1-\frac{(x_U-x_K)}{(x_O-x_K)}\right)*\left(1-\frac{(y_U-y_K)}{(y_O-y_K)}\right)*\left(1-\frac{(x-x_U)}{(x_{1U}-x_U)}\right)*\left(1-\frac{(y-y_U)}{(y_{1U}-y_U)}\right)\end{aligned}, \quad x > x_U$$

$$\begin{aligned}CR_K^1(x,y)=&\left(1-\frac{(x-x_K)}{(x_J-x_K)}\right)*\left(1-\frac{(y-y_K)}{(y_J-y_K)}\right)\\&-\left(1-\frac{(x_T-x_K)}{(x_J-x_K)}\right)*\left(1-\frac{(y_T-y_K)}{(y_J-y_K)}\right)*\left(1-\frac{(x-x_T)}{(x_{0T}-x_T)}\right)*\left(1-\frac{(y-y_T)}{(y_{0T}-y_T)}\right)\end{aligned}, \quad y \le y_T$$

$$\begin{aligned}CR_K^1(x,y)=&\left(\frac{(x-x_K)}{(x_J-x_K)}\right)*\left(1-\frac{(y-y_K)}{(y_J-y_K)}\right)\\&-\left(1-\frac{(x_T-x_K)}{(x_J-x_K)}\right)*\left(1-\frac{(y_T-y_K)}{(y_J-y_K)}\right)*\left(1-\frac{(x-x_T)}{(x_{1T}-x_T)}\right)*\left(1-\frac{(y-y_T)}{(y_{1T}-y_T)}\right)\end{aligned}, \quad y > y_T$$

$$CR_K^2(x,y)=\left(1-\frac{(x-x_K)}{(x_V-x_K)}\right)*\left(1-\frac{(y-y_K)}{(y_V-y_K)}\right) \tag{8}$$

Fig. 12(b) shows the control rate of node K by neglecting the effect due to nodes U and T. Fig. 12(c) shows the control rate of node T in patch 1. Fig. 12(d) shows the control rate of node K after considering the effect due to nodes U and T. The discontinuities of Fig. 12(b) are removed and the control rate of node K at nodes U and T are zero in Fig. 12(d).

4. Experimental Results

We implement the image warping by the control rate derived in section 3. The Nth and (N+1)th frames are shown in Fig. 13(a) and (b) respectively. Figs. 13(a) and (b) show a zooming-in scene in which the ball is rising and the player's right hand is moving up. The mesh with 500 nodes is shown in Fig. 13(c) and the PSNR of the reconstructed frame that is 30.24 db is shown in Fig. 13(d). Figs. 14(a) and (b) show a shifting scene with no moving object. The mesh with 1000 nodes is shown in Fig. 14(c) and the PSNR of the reconstructed frame that is 27.17 db is shown in Fig. 14(d).

5. Conclusion

The quad-tree structure has often been used to decompose an image. Three types of nodes are generated in the quad-tree structure. In this paper, we derived the control rates for these three types of nodes. The warping from a regular mesh can be accomplished by using the control rate of the three types of nodes easily. The image warping from a non-regular mesh can also be accomplished by using the control rate of an intermediate regular mesh with both forward warping and backward warping.

References

[1] G. Al-Regib, Y. Altunbasak and R. M. Mersereau, "Hierarchical Motion Estimation With Content-Based Meshes," ***IEEE Trans. on Circuits and Systems for Video Tech.,*** Vol. 13, No. 10, pp. 1000-1005, October 2003.

[2] P. Hsu, K. J. R. Liu and T. Chen, "A Low Bit-Rate Video Codec Based on Two-Dimensional Mesh Motion Compensation with Adaptive Interpolation," ***IEEE Trans. on Circuits and Systems for Video Tech.,*** Vol. 11, No. 1, pp. 111-117, January 2001.

[3] C. L. Huang and C. Y. Hsu, "A New Motion Compensation Method for Image Sequence Coding Using Hierarchical Grid Interpolation," ***IEEE Trans. on Circuits and Systems for Video Tech.,*** Vol. 4, No. 1, pp. 42-52, February 1994.

[4] ISO/IEC JTC1/SC29/WG N2502a, ISO/IEC 14496-2 Visual, Atlantic City, October 1998.

[5] C. M. Kuo and M. S. Hung, "An Effective Mesh-Based Motion Compensation Technique for Video Coding," ***J. Vis. Commun. Image,*** R.14, pp. 405-427, 2003.

[6] Y. Nakaya and H. Harashima, "Motion Compensation Based on Spatial Transformations," ***IEEE Trans. on Circuits***

and Systems for Video Tech., Vol. 4, No. 3, pp. 339-367, June 1994.

[7] M. Sayed and W. Badawy, “A Novel Motion Estimation Method for Mesh Based Video Motion Tracking,” ***IEEE International Conference on Acoustics, Speech, and Signal Processing, ICASSP,*** pp.337-340, May 2004.

[8] M. Sayed and W. Badawy, “An Affine-Based Algorithm and SIMD Architecture for Video Compression With Low Bit-Rate Applications,” ***IEEE Trans. on Circuits and Systems for Video Tech.,*** Vol. 16, No. 4, pp. 457-471, April 2006.

[9] A. M. Tekalp and Y. Altunbasak, “Closed-Form Connectivity-Preserving Solutions for Motion Compensation Using 2-D Meshes,” ***IEEE Trans. on Image Processing,*** Vol. 6, No. 9, pp. 1255-1269, September 1997.

[10] A. M. Tekalp and Y. Altunbasak, “Occlusion-Adaptive, Content-Based Mesh Design and Forward Tracking,” ***IEEE Trans. on Image Processing,*** Vol. 6, pp. 1270-1280, September 1997.

[11] A. M. Tekalp, P. V. Beek, C. Toklu and B. Gunesl, “Two-Dimensional Mesh-Based Visual-Object Representation for Interactive Synthetic/Natural Digital Video,” ***Proceedings of the IEEE***, Vol. 86, No. 6, pp. 1029-1051, June 1998.

[12] Y. Wang and O. Lee, “Active Mesh — A Feature Seeking and Tracking Image Sequence Representation Scheme,” ***IEEE Trans. on Image Processing,*** Vol. 3, No. 5, pp. 610-624, September 1994.

[13] Y. Wang, O. Lee, and A. Vetro, “Use of Two-Dimensional Deformable Mesh Structures for Video Coding, Part II — The Analysis Problem and a Region-Based Coder Employing an Active Mesh Representation,” ***IEEE Trans. on Circuits and Systems for Video Tech.,*** Vol. 6, No. 6, pp.647-659, December 1996.

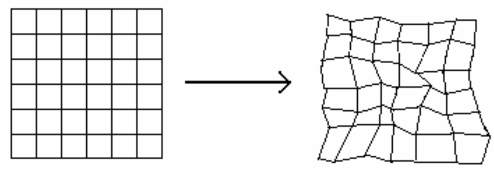

Fig. 1 A deformable mesh

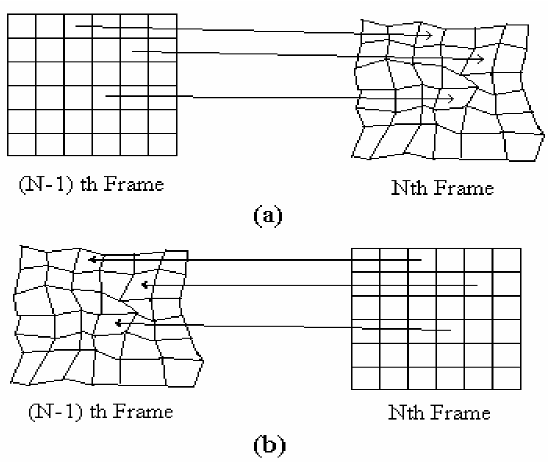

Fig. 2 (a) Forward warping (b) Backward warping

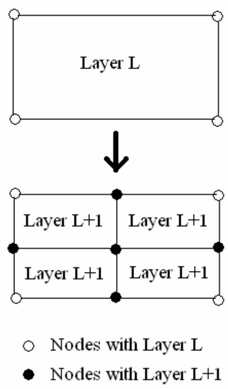

Fig. 3 Illustration of quad-tree decomposition

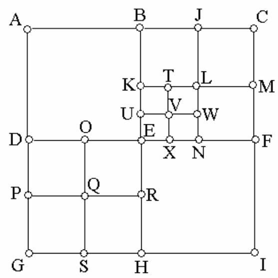

Fig. 4 A mesh in quad-tree representation

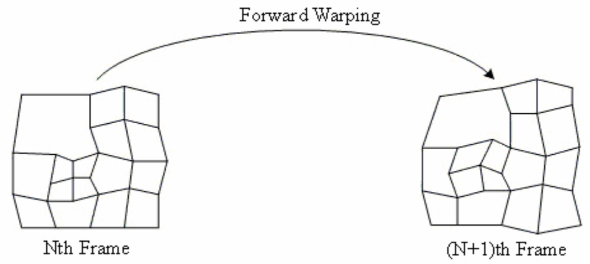

(a)

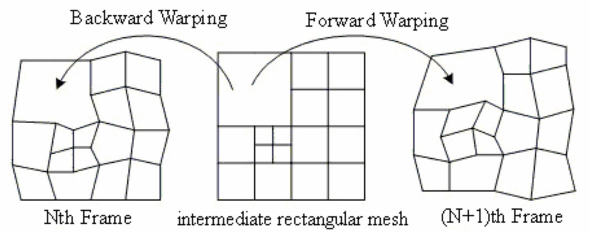

(b)

Fig. 5 (a) Direct image warping between two non-regular meshes.
(b) Indirect image warping between two non-regular meshes.

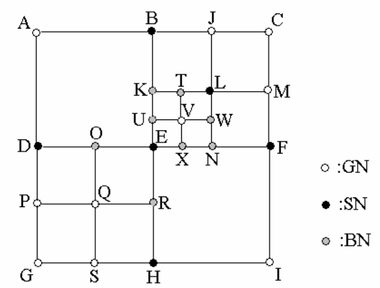

Fig. 6 Three types of nodes defined in the mesh.

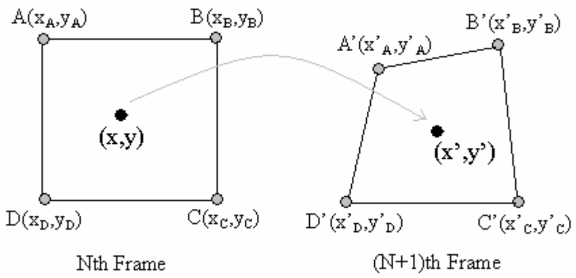

Fig. 7 The warping using bilinear transformation

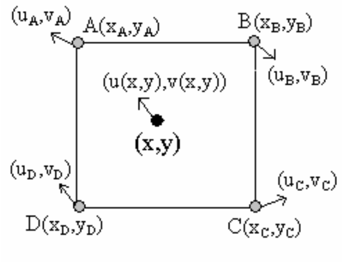

Fig. 8 An example of motion vectors in a patch.

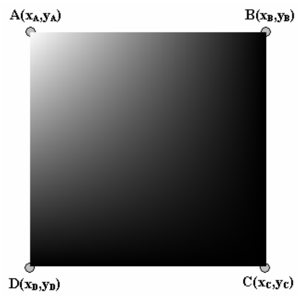

Fig. 9 The control rate of node A within a patch.

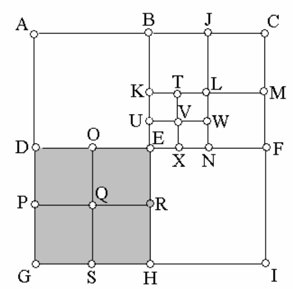

(a)

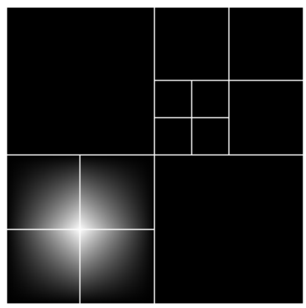

(b)

Fig. 10 (a) The control polygon of GN Q indicated by the gray area.

(b) The control rate of node Q.

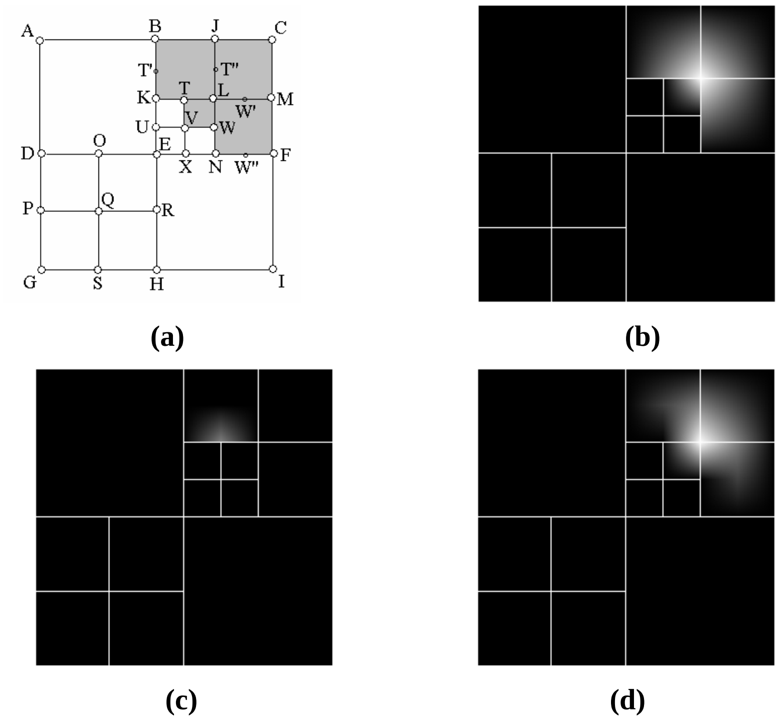

Fig. 11 (a) The control polygon of SN L indicated by the gray area. (b) The initial control rate of node L. (c) The affected quantity of node T. (d) The resulting control rate of node L.

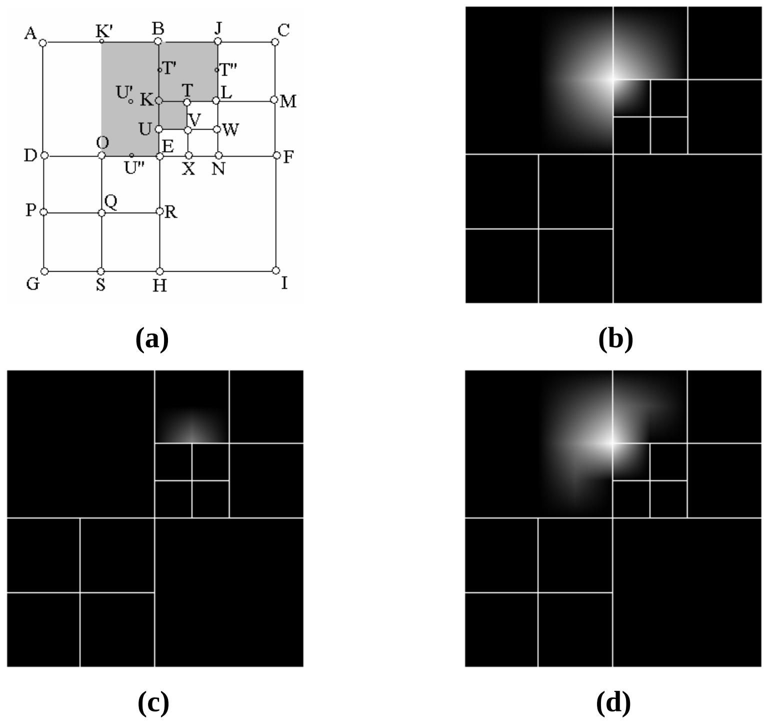

Fig. 12 (a) The control polygon of BN K indicated by the gray area. (b) The initial control rate of node K. (c) The affected quantity of node T (d) The resulting control rate of node K.

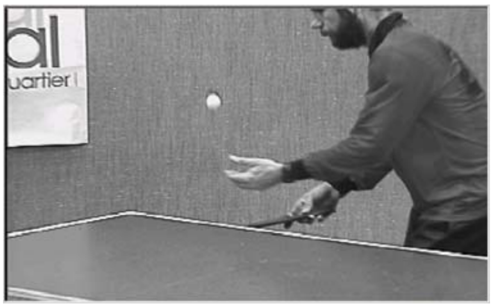

(a) **(b)**

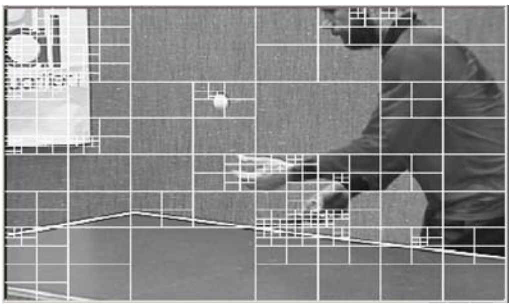

(c) **(d)**

Fig. 13 (a) the Nth frame, (b) the (N+1)th frame, (c) the mesh with 500 nodes, (d) the reconstructed frame

(a) **(b)**

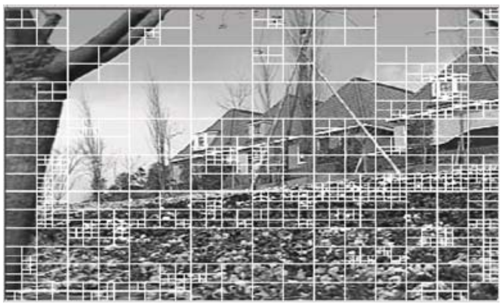

(c) **(d)**

Fig. 14 (a) the Nth frame, (b) the (N+1)th frame, (c) the mesh with 1000 nodes, (d) the reconstructed frame